

On interfacial solitary waves over slowly varying topography

By **KARL R. HELFRICH, W. K. MELVILLE**

Ralph M. Parsons Laboratory, Massachusetts Institute of Technology, Cambridge, MA 02139

AND **JOHN W. MILES**

Institute of Geophysics and Planetary Physics, University of California,
San Diego, La Jolla, CA 92093

(Received 28 October 1983)

The propagation of long, weakly nonlinear interfacial waves in a two-layer fluid of slowly varying depth is studied. The governing equations are formulated to include cubic nonlinearity, which dominates quadratic nonlinearity in some parametric neighbourhood of equal layer depths. Numerical solutions are obtained for an initial profile corresponding to either a single solitary wave or a rank-ordered pair of such waves incident in a monotonic transition between two regions of constant depth. The numerical solutions, supplemented by inverse-scattering theory, are used to investigate the change of polarity of the incident waves as they pass through a 'turning point' of approximately equal layer depths. Our results exhibit significant differences from those reported by Knickerbocker & Newell (1980), which were based on a model equation. In particular, we find that more than one wave of reversed polarity may emerge.

1. Introduction

Recent field observations have provided evidence of packets of long, first-mode internal waves in marginal seas and coastal waters (Osborne & Burch 1980; Apel *et al.* 1975). Such waves may evolve from disturbances caused by tidal flow over topography (e.g. sills and shelf breaks) and propagate for large distances before encountering any further significant variation in bottom topography. Solitary waves may emerge if the propagation distance is large enough. The generation process has been studied in detail (Lee & Beardsley 1974; Maxworthy 1979), but little is known about the ultimate fate of the waves as they propagate towards shore or in regions wherein the depth of the upper layer is a significant fraction of the changing depth of the water column. We consider here one aspect of this problem, the scattering of a solitary wave by a gradually varying change in depth.

Internal solitary waves appear to have been studied originally by Keulegan (1953) (see also Long 1956; Kakutani & Yamasaki 1978), who considered a two-layer liquid with a small discontinuity in density and upper and lower depths of d_+ and d_- and found that the interfacial displacement is positive/negative for $d_+ \gtrless d_-$. This led Kaup & Newell (1978) to suggest that an interfacial solitary wave in water of variable depth could reverse polarity on passing through a transition region in which $d_+ - d_-$ changes sign. Djordjevic & Redekopp (1978) and Miles (1980) have argued that this reversal is impossible if $a/d_- \ll l/L \ll 1$, where a and l are the amplitude and

characteristic length of the wave and L is the length of the transition, but their arguments are inapplicable if $l/L \ll a/d_-$. On the other hand, Knickerbocker & Newell (1980) have shown that such a reversal is possible in the latter case for a model KdV (Korteweg–deVries) equation in which the coefficient of the quadratic term varies linearly over L ; however, their conclusion needs testing for the internal-wave problem in consequence of their neglect of cubic nonlinearity, which dominates quadratic nonlinearity and limits the attainable amplitude of a solitary wave in some neighbourhood of $d_- = d_+$ (Long 1956).

We consider here the formulation and solution of the equations that govern internal solitary waves in a two-layer fluid of gradually varying depth. Significant dimensionless parameters are

$$\alpha = \frac{a}{d}, \quad \beta = \frac{d^2}{l^2}, \quad \delta = \frac{\rho_- - \rho_+}{\rho_- + \rho_+}, \quad \lambda = \frac{l}{L}, \quad (1.1 \ a, b, c, d)$$

where a is a characteristic amplitude (which may be either positive or negative), d is a characteristic depth, l is a characteristic length of the wave, ρ_{\pm} is the density of the upper/lower layer and L is a characteristic length of the depth variation. The parameters α , β and λ are small by hypothesis, and α , which is a measure of nonlinearity, serves as the basic perturbation parameter; the parameter δ may be in $(0, 1)$ but is ultimately assumed to be small.

The parameter β , which measures dispersion, is $O(\alpha)$ for a Boussinesq solitary wave (which represents a balance between quadratic nonlinearity and dispersion); however, $\beta = O(\alpha^2)$ if $|d_- - d_+|/(d_- + d_+) = O(\alpha)$, in which regime cubic nonlinearity is comparable to, or dominates, quadratic nonlinearity.

The parameter λ is assumed to be $O(\beta)$ in the derivation of the generalized KdV equation in §2. If $\lambda \gg \beta$ the effects of variable depth dominate those of nonlinearity and dispersion, and (see §2) a generalization of Green's law holds over the transition region.

We obtain numerical solutions of the resulting evolution equation for a transition between two layers of constant depth (in §4). We also determine asymptotic solutions through the use of inverse-scattering theory (IST), which uses intermediate numerical solutions as initial data, in §5.

2. Evolution equation

Let $y = 0$ be the equilibrium interface, $y = \pm d_{\pm}(x)$ the upper and lower boundaries, $y = y_i(x, t)$ the interfacial displacement, and $\phi(x, y, t)$ the velocity potential (irrotational motion being assumed except at the interface, across which ϕ may be discontinuous). The governing equations, based on the assumptions of incompressible, inviscid flow and continuity of pressure across the interface, are then

$$\nabla^2 \phi = 0 \quad (y \neq y_i), \quad (2.1)$$

$$\phi_y = \pm d'_{\pm} \phi_x \quad (y = \pm d_{\pm}), \quad (2.2)$$

$$\phi_y = y_{it} + \phi_x y_{ix} \quad (y = y_{i\pm}), \quad (2.3)$$

$$\rho_+ \{g y_i + \phi_t + \frac{1}{2}(\nabla \phi)^2\}_{y=y_{i+}} = \rho_- \{g y_i + \phi_t + \frac{1}{2}(\nabla \phi)^2\}_{y=y_{i-}}, \quad (2.4)$$

where the subscripts x, y, t signify partial differentiation, the prime signifies differentiation with respect to x , and, here and subsequently, alternative signs and subscripts are vertically ordered.

The reduction of (2.1)–(2.4) to an evolution equation for y_i may be effected by substituting the expansions†

$$\phi = \{1 \pm y(d_{\pm} \partial_x^2 + d'_{\pm} \partial_x + \frac{1}{3}d_{\pm}^3 \partial_x^4) - \frac{1}{2}y^2 \partial_x^2 + \dots\} \phi_{\pm}(x, t) \quad (y \gtrless y_i), \quad (2.5)_{\pm}$$

which satisfy (2.1) and (2.2)_±, into (2.3)_± and (2.4), and then proceeding as in the derivation of the Korteweg–deVries equation for surface waves (Whitham 1974, §13.11), but retaining both quadratic and cubic nonlinear terms, invoking $ld'_{\pm}/d_{\pm} = O(\lambda)$, and introducing the characteristic variable

$$s = \int \frac{dx}{c} - t. \quad (2.6)$$

The end result is (after dropping the subscript i)

$$d_{-1} c^{\frac{5}{2}} (c^{\frac{1}{2}} y)_x + \frac{1}{6} d_1 y_{sss} + \frac{3}{2} c^2 (d_{-2} y - 2d_{-3} y^2) y_s = 0, \quad (2.7)$$

where

$$d_n = \frac{\rho_- d_-^n + (-)^{n-1} \rho_+ d_+^n}{\rho_+ + \rho_-}, \quad (2.8)$$

$$c = \{g(\rho_- - \rho_+) (\rho_- d_-^{-1} + \rho_+ d_+^{-1})^{-1}\}^{\frac{1}{2}}. \quad (2.9)$$

The wave speed c may be identified as that of infinitesimal, non-dispersive disturbances; cf. Lamb (1932), §231 (11) in the limit $k \downarrow 0$.

The parameter

$$d_0 = \frac{\rho_- - \rho_+}{\rho_- + \rho_+} \equiv \delta \quad (2.10)$$

has the admissible range (0, 1), but typically is small; the boundary condition (2.2)₊ is a valid approximation for a free surface if and only if $\delta \ll 1$. Accordingly, we assume that $\delta \ll 1$ throughout the subsequent development. The corresponding approximations to d_n and c are

$$d_n \rightarrow \frac{1}{2} \{d_-^n + (-)^{n-1} d_+^n\}, \quad c \rightarrow \left\{ \frac{2g\delta d_+ d_-}{d_+ + d_-} \right\}^{\frac{1}{2}} \quad (\delta \downarrow 0). \quad (2.11 a, b)$$

It is convenient to introduce the dimensionless variables

$$\sigma = \frac{c_0 s}{l}, \quad \tau = \frac{1}{6} l^{-3} \int_{x_0}^x d_+ d_- c^{-3} dx, \quad \zeta = \frac{c^{\frac{1}{2}} y}{a}, \quad c = \frac{c}{c_0} \quad (2.12 a, b, c, d)$$

where c_0 is a reference value of c , and transform (2.7) to

$$\zeta_{\tau} + \zeta_{\sigma\sigma\sigma} + 12(\mathcal{U}_1 \zeta - 2\mathcal{U}_2 \zeta^2) \zeta_{\sigma} = 0, \quad (2.13)$$

where

$$\mathcal{U}_1 = \frac{3}{4} \alpha l^2 (d_+ d_-)^{-2} (d_+ - d_-) c^{\frac{3}{2}}, \quad (2.14 a)$$

$$\mathcal{U}_2 = \frac{3}{4} \alpha^2 l^2 (d_+ d_-)^{-3} (d_+^2 - d_+ d_- + d_-^2) c \quad (2.14 b)$$

are measures of quadratic and cubic nonlinearity respectively, relative to dispersion (\mathcal{U}_1 reduces to Ursell's parameter $3\alpha l^2/4d_-^3$ in the limit $\rho_+/\rho_- \downarrow 0$ with d_- fixed). If $\lambda \gtrless \alpha, \beta$ both the dispersion $\zeta_{\sigma\sigma\sigma}$ and nonlinear terms $\zeta \zeta_{\sigma}$ and $\zeta^2 \zeta_{\sigma}$ may be neglected in (2.13), which then yields $\zeta = \text{constant}$ or, equivalently,

$$y \propto c^{-\frac{1}{2}}, \quad (2.15)$$

which is equivalent to Green's law.

† The omitted terms within the brackets are $O(yd^5/l^6, yd^2d'/l^3, y^3d/l^4)$.

3. Solitary-wave solution

Let d be the total depth,

$$d_- = dd, \quad d_+ = (1-d)d \quad (0 < d < 1), \quad (3.1a, b)$$

and choose a (note that $a < 0$ if $d > \frac{1}{2}$) and l according to

$$\alpha = \frac{a}{d} = \frac{2\mu}{1+\mu} \frac{d(1-d)(\frac{1}{2}-d)}{d^3+(1-d)^3}, \quad \frac{1}{\beta} = \frac{l^2}{d^2} = \frac{(1+\mu)^2 d(1-d)\{d^3+(1-d)^3\}}{3\mu(\frac{1}{2}-d)^2}, \quad (3.2a, b)$$

where d is constant and $0 < \mu < 1$; then (2.14) reduce to (with $c \equiv 1$)

$$\mathcal{U}_1 = 1 + \mu, \quad \mathcal{U}_2 = \mu, \quad (3.3a, b)$$

and (2.13) admits the solution (Miles 1979)

$$\eta = \zeta = (\cosh^2 \theta - \mu \sinh^2 \theta)^{-1}, \quad (3.4)$$

where

$$\theta = \sigma - 4\tau = \left[1 - \frac{2\mu(\frac{1}{2}-d)^2}{(1+\mu)^2\{d^3+(1-d)^3\}} \right] \frac{x}{l} - \frac{ct}{l}, \quad (3.5)$$

$$c^2 = 2dg\delta d(1-d). \quad (3.6)$$

Note that $0 < \mu < 1$ implies $\mathcal{U}_1^2 > 4\mathcal{U}_2$.

4. Numerical solutions

Equation (2.13) was solved numerically using the pseudospectral scheme of Fornberg & Whitham (1978). The use of this method is in principle straightforward; however, considerable difficulty was experienced initially with numerical instabilities triggered in the neighbourhood of $d_- = d_+$. The numerical method and its linear stability criterion are presented in the Appendix.

The majority of runs were made for initial data corresponding to a single solitary wave in deep water of depth d propagating towards a cosine-shaped transition to shallow water:

$$d_- = dd \quad (\xi \equiv x/L < 0), \quad (4.1a)$$

$$= d\{d + \frac{1}{2}(d-d_1)[\cos \pi\xi - 1]\} \quad (0 < \xi < 1), \quad (4.1b)$$

$$= dd_1 \quad (\xi > 0), \quad (4.1c)$$

where $d > d_1$. A limited number of runs were conducted for the corresponding transition from shallow to deep water, for linearly varying topography, and for initial data corresponding to a pair of rank-ordered solitary waves.

Figure 1 illustrates the scattering of a single solitary wave moving from deep to shallow water when λ is comparable to α . No solitary waves of reversed polarity emerge.

The example described in figure 2 differs from that of figure 1 only in that $\lambda \ll \alpha$. The plots are presented in a frame moving with the local linear wave speed, and show a lead wave of reversed polarity emerging from the scattered packet on the shelf ($\xi = 1.59$). The profile on the shelf comprises several waves of reversed polarity travelling faster than the linear wave speed. Subsequent IST solutions (§5), using the profile at $\xi = 1.02$ as initial data, show 12 solitary waves emerging on the shelf.

Solitary waves in nature usually occur in a rank-ordered sequence, whence it is of interest to determine whether the evolution of waves of reversed polarity is specific to initial data corresponding to a single solitary wave. The significant dispersion

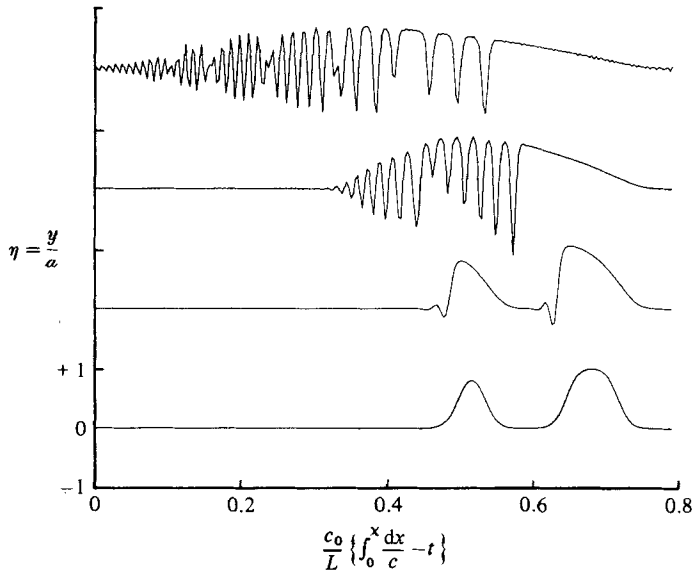


FIGURE 1. Evolution of a single wave of depression over a transition of decreasing depth for $(\alpha_0, \lambda, d, d_1) = (-0.0333, 0.041, 0.6, 0.15)$. Profiles of $\eta = y/a$ are shown as functions of the dimensionless characteristic time $(c_0/L) \{ \int_0^x dx/c - t \}$ at four locations: $\xi = 0, 0.7, 1.02, 1.23$. No solitary waves of elevation emerge.

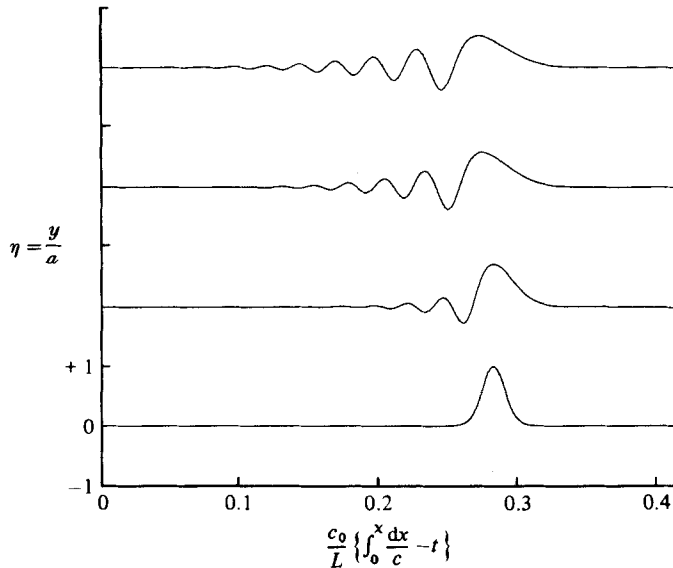


FIGURE 2. Evolution of a single wave of depression over a transition of decreasing depth for $(\alpha_0, \lambda, d, d_1) = (-0.0667, 0.0041, 0.6, 0.15)$. Profiles of η are shown at $\xi = 0, 0.66, 0.95, 1.59$. Note the separation of the leading waves from the scattered packet. IST shows 12 waves of reversed polarity emerging in this case.

evident in figures 1 and 2 implies that two rank-ordered solitary waves separated by a distance $O(l)$ at the bottom of the slope may produce significant interaction in the transition. Figure 3 shows the profiles for such a numerical experiment; waves of reversed polarity are seen to emerge. Comparison of the results of figure 3 with the linear superposition of the solutions for each wave taken separately as initial data

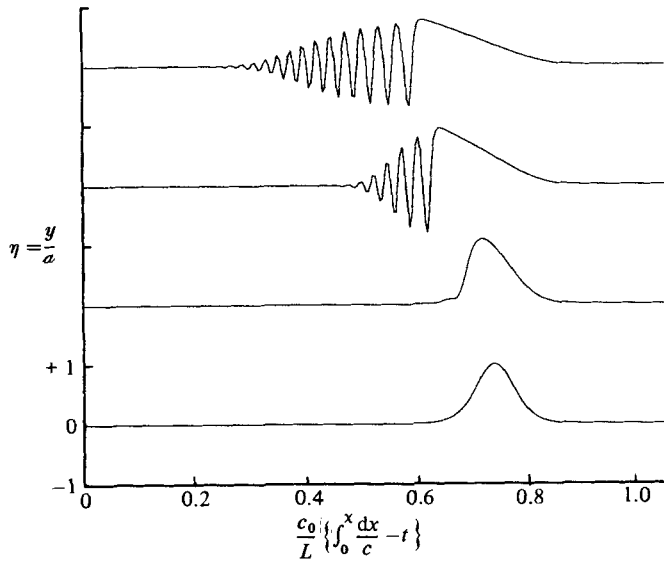


FIGURE 3. Evolution of a pair of rank-ordered solitary waves over a transition of decreasing depth for $(\alpha_{01}, \alpha_{02}, \lambda, d, d_1) = (-0.0833, -0.0667, 0.016, 0.6, 0.2)$. Profiles are shown at $\xi = 0, 0.59, 0.93, 1.28$. As in figure 2, the lead waves are separating from the scattered packet.

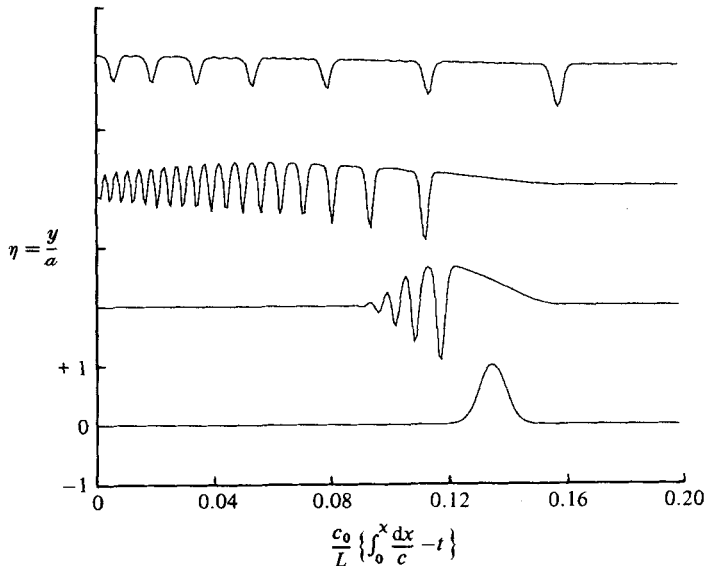


FIGURE 4. Evolution of a single wave of elevation over a transition of increasing depth for $(\alpha_0, \lambda, d, d_1) = (0.0667, 0.0082, 0.333, 1.0)$. Profiles are shown at $\xi = 0, 0.67, 1.02$ and 1.23 . No waves of reversed polarity emerge.

shows that significant interaction remains in the region in which waves of reversed polarity are emerging.

Figure 4 describes a transition from shallow to deep water, with $\lambda \ll \alpha$. There is no evidence of waves of reversed polarity.

For cases in which waves of reversed polarity emerge, our numerical solutions display qualitative differences from those of Knickerbocker & Newell. They attribute the emergence of the wave of reversed polarity to the generation of a shelf behind

the incident solitary wave as it propagates up the slope; however, our results show no significant shelf development with the slope scaling used here. Other numerical experiments (not reported here) show that a very gradual slope is required to obtain a significant shelf: we estimate $\lambda = O(\alpha^n)$, $n = 3-4$, for figure 2 of Knickerbocker & Newell. We conclude that the emergence of the waves of reversed polarity is not attributable solely to the development of a shelf.

5. Asymptotic solutions

The relatively long times required to compute a clear separation of the solitary waves from the scattered packet preclude an extensive study of the asymptotic state on the shelf through numerical integration. If, however, d_+ and d_- are constant, (2.13) can be solved by inverse-scattering theory, and the asymptotic solution on the shelf then can be evaluated using the numerical solution at the top of the slope as initial data.

Following Miles (1981), we set $\mathcal{U}_1 = 2$ and $\mathcal{U}_2 = 1$ in (2.13), which, by virtue of (2.14), is equivalent to choosing appropriate values of a and l . The resulting evolution equation

$$\zeta_\tau + \zeta_{\sigma\sigma\sigma} + 24\zeta(1-\zeta)\zeta_\sigma = 0 \quad (5.1)$$

has solitary-wave solutions

$$\zeta = \frac{2\gamma(1+\gamma)^{-1}}{\cosh^2 \chi - \gamma \sinh^2 \chi} \quad (0 < \gamma < 1), \quad (5.2a)$$

where

$$\chi = \kappa\sigma - 4\kappa^3\tau + \nu, \quad \kappa = 2\gamma^{\frac{1}{2}}(1+\gamma)^{-1}, \quad (5.2b, c)$$

ν is a phase constant, and γ is the family parameter.

Equation (5.1) is reduced to the KdV equation

$$B_\tau + 12BB_\sigma + B_{\sigma\sigma\sigma} = 0 \quad (5.3)$$

through the Miura transformation (Miles 1979),

$$B = \zeta_\sigma + 2\zeta(1-\zeta). \quad (5.4)$$

The asymptotic solution on the shelf is dominated by a discrete set of solitary waves

$$B \sim \sum_1^N \kappa_n^2 \operatorname{sech}^2 \chi_n \quad \text{as } \tau \uparrow \infty, \quad (5.5)$$

where the κ_n are the discrete eigenvalues of

$$\psi''(\sigma) + \{-\kappa^2 + 2B_0(\sigma)\} \psi(\sigma) = 0 \quad (-\infty < \sigma < \infty), \quad (5.6)$$

subject to

$$\psi_n \sim e^{\mp \kappa_n \sigma} \quad \text{as } \sigma \rightarrow \pm \infty, \quad (5.7)$$

and

$$B_0(\sigma) \equiv B(\sigma; \tau_0) = \zeta_\sigma + 2\zeta(1-\zeta)|_{\tau=\tau_0} \quad (5.8)$$

provides the initial data at the top of the shelf ($\tau = \tau_0$).

This eigenvalue problem was solved by expressing (5.6) in centred finite-difference form and evaluating the eigenvalues and eigenvectors by standard methods (Wilkinson 1965; Dahlquist & Björck 1974).

According to inverse-scattering theory, the eigenvalues of (5.6) and (5.7) should be independent of τ , which is a parameter in the scattering problem. As a check on the solution of the eigenvalue problem, we compared the magnitude and number of discrete eigenvalues computed from initial data taken at two positions on the shelf; see table 1 for some typical cases. For transmitted waves comparable in amplitude

| Case | $\xi = 1.02$ | | $\xi = 1.23$ | |
|------|--------------|-----------------------|--------------|------------------------------|
| | N | $-a_T^{(i)}/a_0$ | N | $-a_T^{(i)}/a_0$ |
| (a) | 1 | 0.160 | 2 | 0.155, 0.001 |
| (b) | 2 | 0.216, 0.019 | 2 | 0.201, 0.015 |
| (c) | 3 | 0.369, 0.096 0.012 | 4 | 0.354, 0.083 0.012, 0.001 |
| (d) | 2 | 0.225, 0.006 | 2 | 0.217, 0.006 |

TABLE 1. Number N of transmitted waves and their respective amplitudes relative to the incident-wave amplitude $a_T^{(i)}/a_0$ ($i = 1, \dots, N$), computed by IST from initial data at $\xi = 1.02$ and 1.23 , for the following parameters $(\alpha_0, \lambda, d, d_1)$: (a) $(-0.04, 0.00246, 0.55, 0.368)$; (b) $(-0.033, 0.0082, 0.6, 0.2)$; (c) $(-0.05, 0.0082, 0.6, 0.2)$; (d) $(-0.0667, 0.0041, 0.6, 0.3)$. Note the weak dependence of the results on ξ .

| Case | IST | Numerical |
|------|-------|-----------|
| (a) | 0.941 | 0.911 |
| (b) | 0.725 | 0.695 |
| (c) | 0.369 | 0.371 |

TABLE 2. Asymptotic relative amplitude of first lead wave $(-a_T^{(1)}/a_0)$ from direct numerical solution and from IST using solutions at $\xi = 1.02$ as initial data. The three cases correspond to the following values of parameters $(\alpha_0, \lambda, d, d_1)$: (a) $(-0.0667, 0.0041, 0.6, 0.15)$; (b) $(-0.0833, 0.0041, 0.6, 0.2)$; (c) $(-0.05, 0.0082, 0.6, 0.2)$.

to the incident wave, differences of a few percent in κ_n^2 (and hence the wave amplitude) are observed, with the absolute error remaining of the same order as the wave amplitude decreases. Thus the computed number N of solitary waves may be in error when the amplitude of the smallest eigenvalue approaches that of the error. We were not able to isolate the source of this error, but suspect that it is due in part to the finite resolution of the numerical solution used for initial data.

As a further check on the solution procedures, the numerical solution was run for an extended period in a few cases to provide a direct comparison with the results of the inverse-scattering theory. An example of such a comparison of the largest waves evolving in three separate cases is shown in table 2. The differences between the numerical solutions and the analytical values obtained from IST are less than 5% for lead waves whose amplitudes are comparable to those of the incident waves. These differences are comparable with those cited above for the errors in the implementation of the IST.

Numerical solutions through the transition region, supplemented by IST, were used to explore a larger parameter space than was practicable with the direct numerical solutions alone. Figure 5 shows the number of transmitted solitary waves versus λ , the transition-length parameter, for fixed values of the incident-wave amplitude, and displays an increase in the number of waves as λ decreases (the length of the transition increases).† The results of figure 5 were used to determine the wave amplitude at transition between $N = 0, 1$ and $N = 1, 2$, as shown in figure 6. The transition from

† Some of the results in this section were obtained with a higher-order contribution to \mathcal{Q}_0 in (2.13). With amplitudes of the transmitted waves differing by 1–2%, this additional term made no significant difference to the asymptotic results.

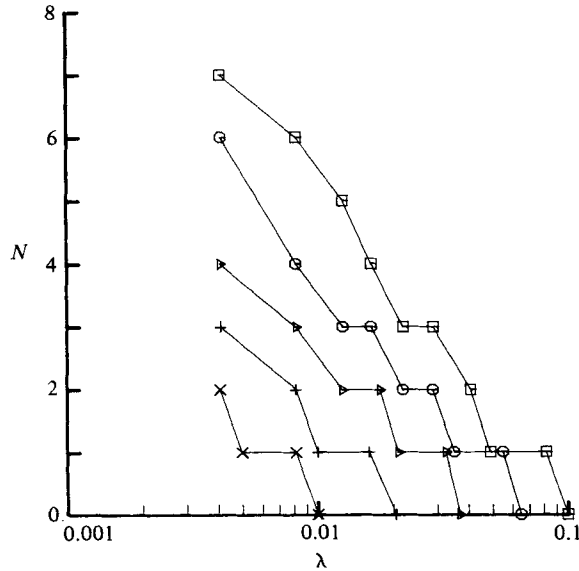


FIGURE 5. Number N of transmitted solitary waves versus λ for fixed values of $d = 0.6$ and $d_1 = 0.2$, and incident amplitudes $\alpha_0 = -0.0833$ ($-\square-$); -0.0667 ($-\circ-$); -0.05 ($-\triangleright-$); -0.0333 ($-\+-$); -0.0167 ($-\times-$).

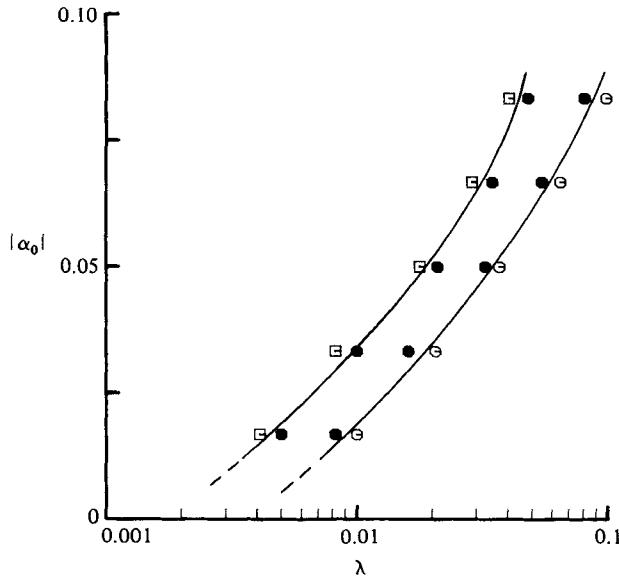


FIGURE 6. Incident-wave amplitudes α_0 at transitions between $N = 0, 1$ and $N = 1, 2$ versus the slope-length parameter λ , obtained from the data in figure 5. \circ , $N = 0$; \bullet , 1 ; \square , 2 .

$N = 0, 1$ occurs for $|\alpha_0|$ increasing through a value comparable with λ . Similar results, in figures 7 and 8, show that for a smaller depth change a larger incident wave is required to initiate a wave of reversed polarity.

Figure 9 shows the amplitude of the first transmitted solitary wave versus the amplitude of the incident wave for λ in the range $[0.0041, 0.041]$. Our results show that the amplitude of the first transmitted wave increases as λ decreases. This contrasts with the results of Knickerbocker & Newell (1980), which show an

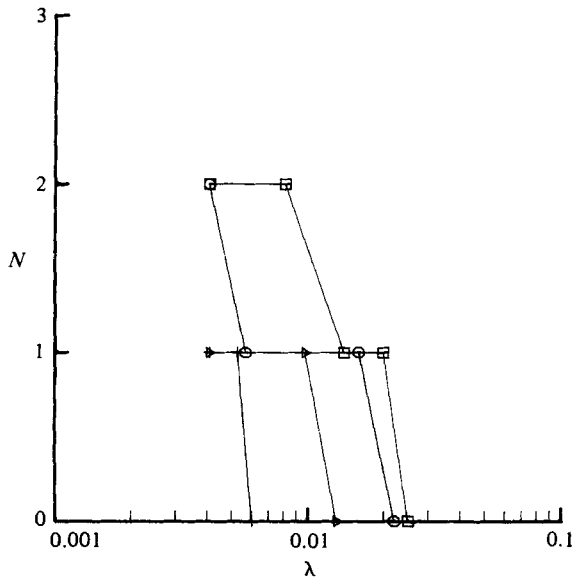


FIGURE 7. as in figure 5, except $d = 0.6$, $d_1 = 0.3$.

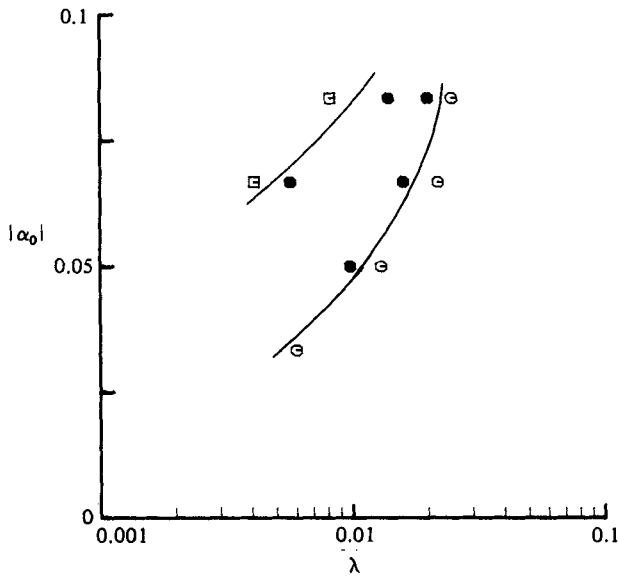


FIGURE 8. As in figure 6 with transition data obtained from figure 7.

asymptotic regime, independent of the transition lengthscale, in which $\alpha_T = \frac{1}{3}\alpha_0$, where α_0 and α_T are the dimensionless amplitudes of the incident and transmitted solitary waves respectively (note that Knickerbocker & Newell found only one transmitted wave in their numerical solutions).

A limited study of the sensitivity of the results to the topographic shape was conducted. The results for the same depth change are shown in table 3 for a cosine transition of half-wavelength L , a linear transition of length L and a linear transition of length $2L/\pi$. The last corresponds to a slope equal to the maximum slope of the cosine transition. The differences in amplitude of the lead wave are greater than the

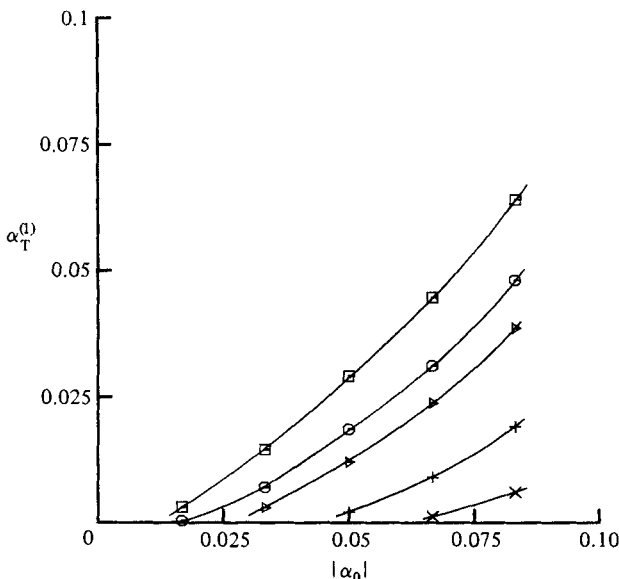


FIGURE 9. Amplitude α_T of first transmitted solitary wave versus the amplitude α_0 , of the incident wave for $d = 0.6$, $d_1 = 0.2$. —□—, $\lambda = 0.0041$; —○—, 0.0082; —▷—, 0.0123; —+—, 0.0225, —×—, 0.041.

| Shape | N | $-\alpha_T^{(i)}/\alpha_0$ |
|-----------------------------|-----|----------------------------|
| (a) Half-cosine length L | 3 | 0.28, 0.09, 0.02 |
| (b) Linear, length L | 2 | 0.39, 0.11 |
| (c) Linear, length $2L/\pi$ | 2 | 0.22, 0.01 |

TABLE 3. Dependence of transmitted-wave amplitude on transition geometry $(\alpha_0, \lambda, d, d_1)$ = $(-0.0667, 0.016, 0.6, 0.2)$ from IST using initial data at $\xi = 1.02$

errors discussed above and suggest that the details of the topography may be significant in the application of these results.

A number of runs were conducted without the cubic term. Over the range of parameters studied we found quantitative rather than qualitative differences from those solutions which included the effects of cubic nonlinearity. The differences were most pronounced in the neighbourhood of the slope and less so in the asymptotic results on the shelf. Laboratory experiments (which will be reported later) show that the inclusion of cubic nonlinearity provides a significantly improved prediction of the wave profiles over gradual slopes.

The authors wish to thank Dr Daniel Meiron for a helpful conversation on eigenvalue solvers. This work was supported by the National Science Foundation with an award of computer time at the National Center for Atmospheric Research and Grants OCE 77-24005 (UCSD) and OCE-81-17539 (UCSD), and by contracts (at both MIT and UCSD) with the Office of Naval Research.

Appendix

Equation (2.13) was solved using the explicit pseudospectral method of Fornberg & Whitham (1978)†. The method evaluates the σ -derivatives of $\zeta(\sigma, \tau)$ in Fourier space, and steps forward in τ using a leapfrog procedure. For the constant-coefficient KdV equation

$$u_\tau + uu_\sigma + u_{\sigma\sigma\sigma} = 0 \quad (\text{A } 1)$$

this gives

$$u_j^{m+1} - u_j^{m-1} + 2i \Delta\tau u_j^m \mathcal{F}^{-1}\{k \mathcal{F}(u^m)\} - 2i \mathcal{F}^{-1}\{\sin(k^3 \Delta\tau) \mathcal{F}(u^m)\} = 0, \quad (\text{A } 2)$$

where

$$u_j^m = u(j \Delta\sigma, m \Delta\tau),$$

$$k = \frac{2\pi}{N \Delta\sigma} \nu \quad (\nu = 0, \pm 1, \dots, \pm \frac{1}{2}N),$$

and \mathcal{F} and \mathcal{F}^{-1} represent the forward and inverse Fourier transforms respectively.

Using the same procedure for (2.13), we obtain

$$\zeta_j^{m+1} - \zeta_j^{m-1} + 24i \Delta\tau (\mathcal{U}_1^m \zeta_j^m - 2\mathcal{U}_2^m \zeta_j^m) \zeta_j^m \mathcal{F}^{-1}\{k \mathcal{F}(\zeta^m)\} - 2i \mathcal{F}^{-1}\{\sin(k^3 \Delta\tau) \mathcal{F}(\zeta^m)\} = 0. \quad (\text{A } 3)$$

A numerical stability criterion for (A 3) may be approximated by considering the linear equation

$$\zeta_\tau + A \zeta_\sigma + \zeta_{\sigma\sigma\sigma} = 0 \quad (\text{A } 4)$$

with A constant. Following FW, (A 4) has the stability condition

$$\left| \pm \sin \left[\left(\frac{\pi}{\Delta\sigma} \right)^3 \Delta\tau \right] - \frac{\pi}{\Delta\sigma} A \Delta\tau \right| < 1. \quad (\text{A } 5)$$

This condition is generalized for (2.13) by setting

$$A = 12(\mathcal{U}_1 \zeta - 2\mathcal{U}_2 \zeta^2), \quad \text{or} \quad A \approx 12(\mathcal{U}_1 - 2\mathcal{U}_2),$$

since $\zeta \leq 1$. The maximum of $|\mathcal{U}_1 - 2\mathcal{U}_2|$ occurs on the shelf when $\mathcal{U}_1 < 0$, so that (A 5) becomes

$$\left| \sin \left[\left(\frac{\pi}{\Delta\sigma} \right)^3 \Delta\tau \right] - \frac{\pi}{\Delta\sigma} 12(\mathcal{U}_1 - 2\mathcal{U}_2)_{\text{shelf}} \right| < 1. \quad (\text{A } 6)$$

The condition (A 6) may be very restrictive, since it is determined from $(\mathcal{U}_1 - 2\mathcal{U}_2)_{\text{shelf}}$, which in some cases may be an order of magnitude larger than $\mathcal{U}_1 - 2\mathcal{U}_2$ prior to the slope. To alleviate this problem and optimize the time step $\Delta\tau$, we have added and subtracted a dummy advective term $C_a \zeta_\sigma$ in (A 3), where C_a is a constant. The numerical approximation then becomes

$$\zeta_j^{m+1} - \zeta_j^{m-1} + 24i \Delta\tau (\mathcal{U}_1^m \zeta_j^m - 2\mathcal{U}_2^m \zeta_j^{m2} + C_a) \mathcal{F}^{-1}\{k \mathcal{F}(\zeta^m)\} - 2i \mathcal{F}^{-1}\{\sin(k^3 \Delta\tau + C_a k \Delta\tau) \mathcal{F}(\zeta^m)\} = 0, \quad (\text{A } 7)$$

and the stability condition is modified to

$$\left| \pm \sin \left[\left(\frac{\pi}{\Delta\sigma} \right)^3 \Delta\tau + \frac{\pi}{\Delta\sigma} C_a \Delta\tau \right] - \frac{\pi}{\Delta\sigma} \Delta\tau [12(\mathcal{U}_1 - 2\mathcal{U}_2) + C_a] \right| < 1. \quad (\text{A } 8)$$

The constant C_a is chosen so that $\Delta\tau$ is maximized and (A 8) is satisfied during the entire run.

† Abbreviated to FW in this appendix.

As a check of the numerical solutions, the integral invariants of (2.13),

$$\frac{\partial}{\partial \tau} \int_{-\infty}^{\infty} \zeta \, d\sigma = 0 \rightarrow \sum_{j=1}^N \zeta_j^m = \text{constant}$$

and

$$\frac{\partial}{\partial \tau} \int_{-\infty}^{\infty} \zeta^2 \, d\sigma = 0 \rightarrow \sum_{j=1}^N (\zeta_j^m)^2 = \text{constant},$$

were calculated. Variations in these quantities over the duration of a run were within $\pm 0.1\%$ of the initial values for most cases and within $\pm 1\%$ in the worst case.

In order to compute solutions at large values of ξ , it was necessary in some cases to expand the σ -domain from 256 to 512 grid points. This prevented the tail of the scattered packet from wrapping around (in consequence of the periodic boundary conditions). For a few runs, repeated grid expansion would have required excessive computational time; in these situations the tail of the scattered packet was truncated with a tanh window. The effect of truncation on the asymptotic solutions was tested using IST theory. IST solutions for the asymptotic conditions were performed on untruncated and truncated initial data. No effect on the IST results were observed until the initial data were truncated within $N+2$ waves from the front of the packet, where N is the number of discrete eigenvalues found from the truncated solution. Figure 2 is an example of a run in which the grid was expanded and the tail truncated. Only the central 256 grid points are shown in the figure; the truncation is not shown.

REFERENCES

- APEL, J. R., BYRNE, H. M., PRONI, J. R. & CHARNELL, R. L. 1975 Observation of oceanic internal and surface waves from the Earth Resources Technology Satellite. *J. Geophys. Res.* **80**, 865–881.
- DAHLQUIST, G. & BJÖRCK, A. 1974 *Numerical Methods*. Prentice-Hall.
- DJORDJEVIC, V. D. & REDEKOPP, L. G. 1978 The fission and disintegration of internal solitary waves moving over two-dimensional topography. *J. Phys. Oceanogr.* **8**, 1016–1024.
- FORNBERG, B. & WHITHAM, G. B. 1978 A numerical and theoretical study of certain nonlinear wave phenomena. *Phil. Trans. R. Soc. Lond. A* **289**, 373–404.
- KAKUTANI, T. & YAMASAKI, N. 1978 Solitary waves on a two-layer fluid. *J. Phys. Soc. Japan* **45**, 674–679.
- KAUP, D. J. & NEWELL, A. C. 1978 Solitons as particles, oscillators, and in slowly changing media: a singular perturbation theory. *Proc. R. Soc. Lond. A* **361**, 413–446.
- KEULEGAN, G. H. 1953 Characteristics of internal solitary waves. *J. Res. Natl Bur. Standards* **51**, 133–140.
- KNICKERBOCKER, C. J. & NEWELL, A. C. 1980 Internal solitary waves near a turning point. *Phys. Lett.* **75 A**, 326–330.
- LAMB, H. 1932 *Hydrodynamics*. Cambridge University Press.
- LEE, C. Y. & BEARDSLEY, R. C. 1974 The generation of long nonlinear internal waves in a weakly stratified shear flow. *J. Geophys. Res.* **79**, 453–462.
- LONG, R. R. 1956 Solitary waves in one- and two-fluid systems. *Tellus* **8**, 460–471.
- MAXWORTHY, T. 1979 A note on the internal solitary waves produced by tidal flow over a three-dimensional ridge. *J. Geophys. Res.* **84**, 338–346.
- MILES, J. W. 1979 On internal solitary waves. *Tellus* **31**, 456–462.
- MILES, J. W. 1980 Solitary waves. *Ann. Rev. Fluid Mech.* **12**, 11–43.
- MILES, J. W. 1981 On internal solitary waves, II. *Tellus* **33**, 397–401.
- OSBORNE, A. R. & BURCH, T. L. 1980 Internal solitons in the Andaman Sea. *Science* **208**, 451–460.
- WHITHAM, F. B. 1974 *Linear and Nonlinear Waves*. Academic.
- WILKINSON, J. H. 1965 *The Algebraic Eigenvalue Problem*. Clarendon.